Dynamics of ions of the two-dimensional superionic conductor $AgCrS_2$

P. Brüesch and T. Hibma
Brown-Boveri Research Center, CH-5405 Baden, Switzerland

W. Bührer
Institut für Reaktortechnik, Eidenössische Technische Hochschule Zürich, CH-5303 Würenlingen, Switzerland

(Received 20 October 1982)

$AgCrS_2$ is a quasi-two-dimensional superionic conductor for silver ions which shows a second-order phase transition at $T_c = 673$ K. Well below T_c, $AgCrS_2$ is ordered and pyroelectric; above T_c the silver ions are disordered and the phase is nonpyroelectric. The ion dynamics below T_c has been studied by means of far-infrared and inelastic neutron scattering experiments. The most interesting feature of the phonon structure is the existence of very-low-frequency acoustic and flat optic modes. The low-frequency TO mode at $q=0$ shows a strong and anomalous temperature dependence down to 10 K. We show that this temperature dependence can be explained by a highly anharmonic motion of a particle in an effective potential. The patterns of ionic displacements of the low-frequency modes have been obtained from a calculation based on a rigid-ion model. This calculation shows that in the low-frequency modes the silver ions are strongly involved and vibrate parallel to the layers. These modes therefore contribute strongly to the mean-square displacements of the silver ions and to the reaction coordinates for ionic jumps. The jumps of silver ions reduce the spontaneous polarization of the pyroelectric phase and finally lead to the order-disorder pyroelectric phase transition at T_c.

I. INTRODUCTION

$AgCrS_2$ is a member of the large family of silver-based superionic conductors such as AgI, Ag_2S, Ag_3SI, $RbAg_4I_5$, Ag_2HgI_4, and $(C_5H_5NH)Ag_5I_6$.[1,2] One of the interesting features of $AgCrS_2$ lies in the fact that it is a layer structure in which the conducting silver ions are constrained to move in essentially two-dimensional planes. This is shown in Fig. 1 which represents the rhombohedral unit cell (space group C_{3v}^5) together with the stacking of the Cr, S, and Ag layers.[3-5] The silver ions occupy tetrahedral sites in the so-called "van der Waals gap" formed by the sulfur layers. These sites form a pseudo-two-dimensional puckered honeycomb lattice, only half of which are occupied. At low temperatures the silver ions are ordered on one of the triangular sublattices (denoted by α in Fig. 1), but at higher temperatures a disordering over both sublattices α and β takes place gradually and leads to a second-order phase transition at $T_c = 673$ K (Refs. 6 and 7) (space group D_{3d}^5).

There is another interesting aspect: Single domain crystals of $AgCrS_2$ in the low-temperature phase are pyroelectric due to the fact that the α sites occupied by Ag ions are not exactly located midway between the adjacent sulfur planes but shifted by about 0.25 Å in the z direction (Fig. 1). This leads to a static dipole moment in the z direction. Above T_c, $AgCrS_2$ is nonpyroelectric because the α and β sites are occupied with equal probability. Thus the phase transition from a normal ionic conductor to a superionic conductor is simultaneously an order-disorder pyroelectric phase transition.

The ionic and electronic part of the conductivity of this material has been measured before.[8] Below the phase transition the ionic conductivity increases much faster than exponential because of the disordering process. At T_c a sudden change in the slope of the $\log(\sigma T)$ vs $1/T$ curve is observed. The electronic part of the conductivity is much smaller than the ionic part, except at very high temperatures; this is due to the fact that the valence electrons are localized at the chromium ions.[3] The λ-type anomaly observed in $c_p(T)$ (Ref. 7) as well as the absence of a discontinuity in the electronic and ionic conductivity confirm the second-order nature of the transition.

The aim of this paper is to study the dynamical properties of this two-dimensional superionic conductor by means of far-infrared optical techniques and inelastic neutron scattering experiments. The knowledge of the ion dynamics is crucial for the understanding of the mechanism of ionic conductivity in superionic conductors. The instantaneous

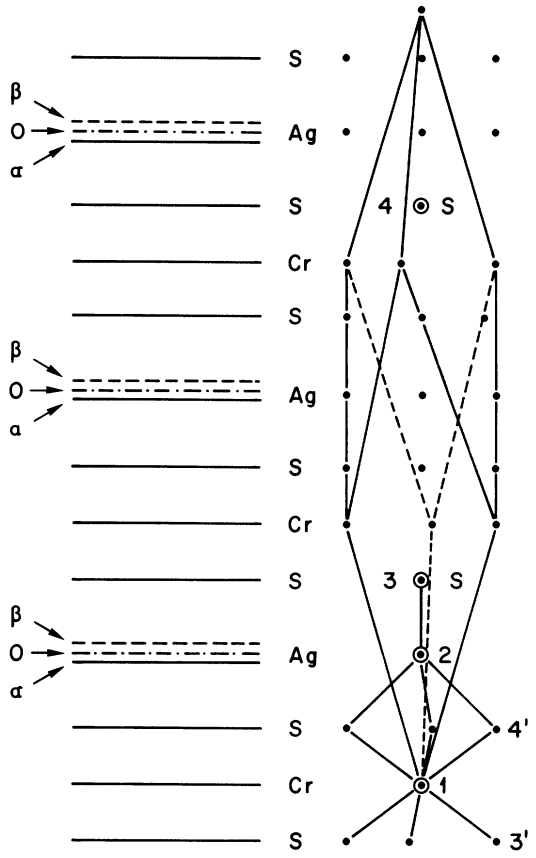

FIG. 1. Rhombohedral unit cell of $AgCrS_2$ containing the four ions 1, 2, 3, and 4. The figure also shows the stacking of the Cr, S, and Ag layers. At low temperatures the Ag ions occupy only the α sites, but above $T_c = 673$ K the α and β sites are occupied with equal probability. The planes marked with O are midway between the S layers and contain empty octahedral sites.

position of a conducting ion relative to its neighbors is of central interest in the diffusion process and represents a suitable reaction coordinate for ionic jumps which can be expressed in terms of the phonon structure (eigenvectors, density of states).[9] Evidently, low-frequency, flat optic modes and low-frequency, acoustic zone-boundary modes give the main contributions to the reaction coordinate, because they have large vibrational amplitudes, high density of states, and are easily thermally activated. In the phonon spectrum of $AgCrS_2$ we indeed observe such flat and low-frequency optic and acoustic modes. Lattice-dynamical calculations show that the silver ions are strongly involved in all these modes. In particular, there exist zone-boundary acoustic modes in which neighboring silver ions in a plane move in opposite directions while the S and Cr ions do not move. Such modes will provide particularly large contributions to the reaction coordinate.

The low-frequency TO mode observed in the far-infrared and inelastic neutron scattering spectra shows a very pronounced and anomalous softening with increasing temperature. This softening is unique in the large family of Ag-based superionic conductors and reflects a highly anharmonic motion of the silver ions down to very low temperatures.

In Sec. II we present the far-infrared optical measurements and the inelastic neutron scattering experiments. In Sec. III we give an interpretation of the experimental data on the basis of lattice-dynamical calculations. Furthermore, it is shown that the unusual and strong temperature dependence of the low-frequency far-infrared mode can be accounted for by considering the motion of a single particle in an effective anharmonic potential. Finally, we discuss the experimental and theoretical results in relation with the ionic conductivity and the order-disorder transition.

II. EXPERIMENTAL

Single-phase $AgCrS_2$ powder was prepared by heating the elements in an evacuated silica tube at 1000 °C for several days and cooling down slowly. Excess sulfur was removed by treating the samples with CS_2. From the freshly prepared powder, tablets were pressed and then polished before measuring the reflectivity. Single crystals of $Ag_{1-x}CrS_{2-x}Cl_x$ ($x=0.03$) in the form of thin platelets were grown by adding a small amount of $CrCl_3$ to $AgCrS_2$ powder. This mixture was sealed under vacuum in a quartz ampule and kept at a temperature of 1000 °C for eight weeks. A comparison between the far-infrared spectra of the tablets and of the single crystals shows that the small amount of Cl present in the latter does not give rise to measurable changes in the vibrational properties.

All far-infrared measurements have been performed with a Beckman FS 720 interferometer. For measurements above 150 cm^{-1} the instrument was used in the Michelson mode and below 150 cm^{-1} in the polarizing mode.[10] The measurements were performed with a dc mercury source and a Golay detector. Most spectra were recorded with a resolution between 3 and 6 cm^{-1}. A specially constructed reflection and transmission cell was used in the temperature range from 133 to 723 K.[11] In addition, reflectivity measurements on $AgCrS_2$ tablets were performed between 16 K and room temperature using an Oxford CF 204 continuous-flow cryostat.

The phonon dispersion of the lowest-energy modes as well as the temperature dependence of selected phonon modes between 4 and 300 K was determined by coherent inelastic neutron scattering techniques on a small but perfect single crystal of

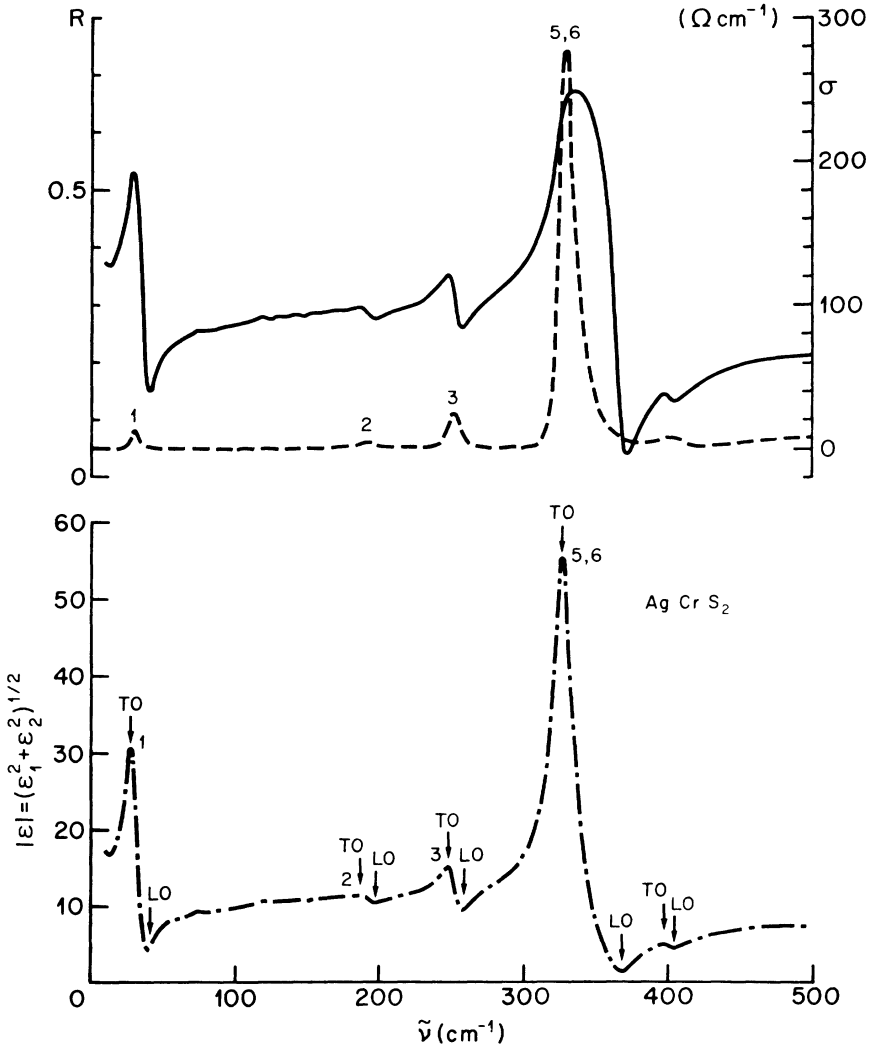

FIG. 2. Far-infrared reflectivity (—), conductivity (— — —), and modulus of the dielectric constant (— · — · —) at room temperature of $AgCrS_2$ pellets. The numbers of the peaks refer to Table I.

$Ag_{1-x}CrS_{2-x}Cl_x$ ($x=0.03$). For the experiments the triple-axis spectrometer at the Saphir reactor was used in its doubly focusing mode of operation.[12]

Figure 2 shows the far-infrared reflectivity of a $AgCrS_2$ pellet at room temperature. Note the low-frequency structure near 30 cm^{-1}. As will be discussed later, this structure originates from a vibration of the Ag layers against the rigid S-Cr-S layers parallel to the direction of the layers (Figs. 3 and 7). The structures above 200 cm^{-1} are due to vibrations

TABLE I. Observed and calculated frequencies of the infrared-active modes. All frequencies are in units of cm^{-1} (see Fig. 2).

Mode No.	Observed $\tilde{\nu}_{TO}$	Observed $\tilde{\nu}_{LO}$	Polarization	Calculated $\tilde{\nu}_{TO}$	Calculated $\tilde{\nu}_{LO}$
1	30	39	$\perp z, E$	32.7	41.5
2	187	196	$\parallel z, A_1$	119.8	122.2
3	246	258	$\perp z, E$	216.0	216.3
4			$\parallel z, A_1$	312	313
5	326	~366	$\perp z, E$	302.8	366.6
6	320–360[a]		$\parallel z, A_1$	315.8	377.4

[a]Overlapping with mode 5.

involving sulfur and Cr ions. Figure 2 also gives the frequency-dependent conductivity $\sigma(\tilde{\nu})$ as obtained from a Kramers-Kronig analysis of the reflectivity data, and the frequency dependence of the modulus of the dielectric constant $|\epsilon| = (\epsilon_1^2 + \epsilon_2^2)^{1/2}$, together with the TO and LO frequencies.[13] The assignment of the peaks (polarization $||z, A_1$ and $\perp z, E$, where z is the trigonal axis) in Table I is based on independent reflectivity and transmission measurements performed on single crystals. In Fig. 3 the temperature dependence of the absorption coefficient $\alpha(\tilde{\nu})$ of the low-frequency mode is depicted. These results have been obtained from transmission measurements of a thin $Ag_{1-x}CrS_{2-x}Cl_x$ single crystal ($x=0.03$) with the cross section perpendicular to the trigonal z axis. The mode softens considerably with increasing temperature. Note that the shape of the absorption band is asymmetric and that above 373 K the absorption on the low-frequency side increases with increasing temperature which results in a pronounced shoulder at 573 and 723 K. If these shoulders are subtracted from the main absorption bands, the linewidth of the latter is only weakly temperature dependent. Figure 4 shows the temperature dependence of the low-frequency TO mode at the Γ point as obtained from the far-infrared[14] and inelastic neutron scattering experiments. The relative frequency change $\Delta\tilde{\nu}/\tilde{\nu}(10\text{ K})$ is as large as 42% between 10 K and $T_c = 673$ K. There is no anomaly at T_c. Note also the unusual shape of the $\tilde{\nu}(T)$ curve at low temperatures: $\tilde{\nu}(T)$ shows a strong decrease already at low temperatures and a change in slope near 200 K. Figure 4 also shows that the linewidth of this mode obtained from inelastic neutron and far-infrared experiments is large and practically temperature independent from 50 K up to room temperature and increases only slightly at higher temperatures. In contrast to the strong temperature dependence of $\tilde{\nu}_{TO}$, the frequency $\tilde{\nu}_{TA}$ at the T point [Fig. 5(a)] is nearly independent of temperature between 50 and 300 K (Fig. 4). Figure 5 contains the observed and calculated phonon dispersion of the TA, LA, and low-frequency TO modes propagating along the trigonal axis (Γ-T). Figure 6 contains the same information for acoustic modes propagating along Γ-L and Γ-X.

III. INTERPRETATION AND DISCUSSION

A. Phonon dispersion from the rigid-ion model

The space group of $AgCrS_2$ is C_{3v}^5 ($R\,3m$); the primitive trigonal unit cell (Fig. 1) contains one formula unit with all atoms in positions with site symmetry C_{3v}. A factor-group analysis leads to the following representation of the $q=0$ modes:

$$\Gamma = 4A_1 + 4E \,. \tag{1}$$

Both the A_1 and E modes are infrared active. The A_1 vibrations are polarized parallel to the trigonal z axis, while the doubly degenerate E modes are polarized perpendicular to z. After subtracting the three translational motions of the crystal we expect $3A_1$

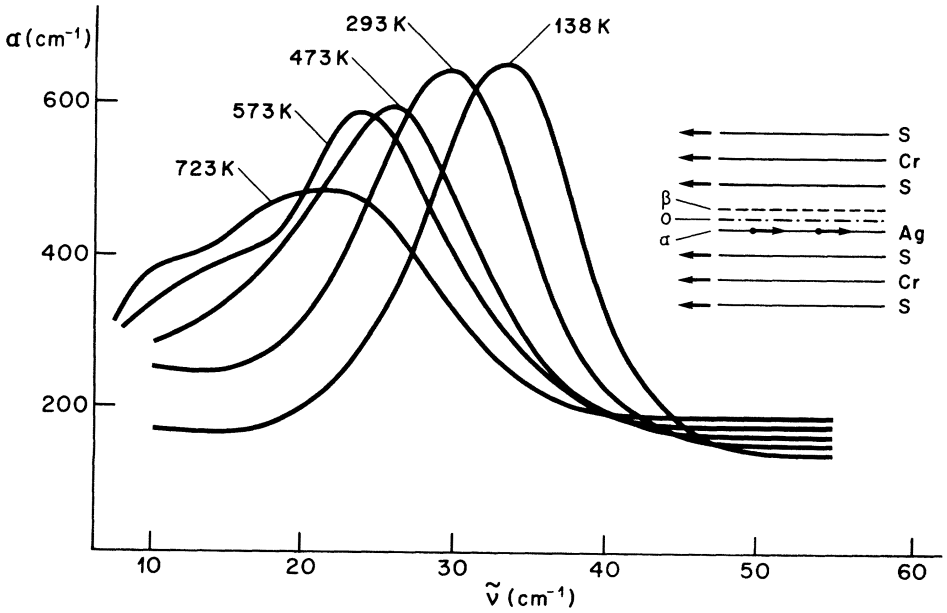

FIG. 3. Absorption coefficient of the low-frequency TO mode as obtained from far-infrared transmission on a thin single crystal. The phase transition temperature is at 673 K. The inset shows the pattern of ionic displacements of this mode.

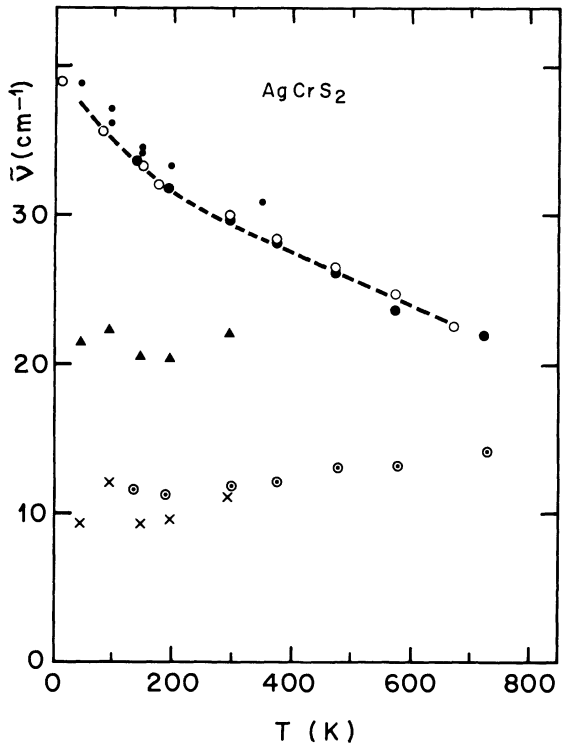

FIG. 4. Temperature dependence of the frequency $\tilde{\nu}_{TO}$ and width Γ_{TO} of the low-frequency TO mode at $q=0$, and of the frequency $\tilde{\nu}_{TA}$ of the TA mode at the T point of $AgCrS_2$. $\tilde{\nu}_{TO}(T)$: ○ from far-infrared reflectivity on pellets, ● from far-infrared transmission on single crystals, • from inelastic neutron scattering on single crystals. $\Gamma_{TO}(T)$: ⊙ from far-infrared transmission on a single crystal, × from inelastic neutron scattering. $\tilde{\nu}_{TA}$: ▲ from inelastic neutron scattering. The dashed line represents the model calculation (see text).

and $3E$ phonons in the infrared spectrum.

The potential energy for an arbitrary wave vector $\vec{q}$ is written as[15]

$$V=V_s+V_c\ , \tag{2}$$

where V_s is the short-range part due to the overlap forces between nearest ions, and V_c is the long-range Coulomb interaction. The complicated force field of $AgCrS_2$ requires the introduction of ten different short-range interactions which are listed in Table II. For the Coulomb interactions the dynamical effective charges used for the calculations are $q_{Cr}=1.2e$, $q_{Ag}=0.3e$, and $q_S=-0.75e$. The fitted model gives good agreement with the experimental phonon dispersion shown in Figs. 5 and 6. These figures also contain approximate patterns of ionic displacements for specific zone-center and zone-boundary modes, which have been calculated on the basis of the model. Figure 7 shows approximate patterns of ionic displacements for the $q=0$ modes. The model correctly predicts the existence of low-frequency modes in which the silver ions are strongly involved, and high-frequency optical modes which involve relative motions of chromium against sulfur ions. There exist, however, considerable discrepancies between observed and calculated frequencies especially for mode 2. This discrepancy is connected with the large anisotropy in the vibrational frequencies of modes 1 and 2 (Fig. 7, Table I). Large anisotropies in the force constants for corresponding modes polarized parallel and perpendicular to the z axis have been observed in layer compounds with the $CdCl_2$ and $Cd(OH)_2$ structure and have been explained on the basis of a model which includes the effect of the static dipole moments of the anions on the force constants.[16–18] The results of this model cannot, however, be directly applied to the different and more complicated structure of $AgCrS_2$. In $AgCrS_2$ the silver ions are not located exactly between the sulfur planes but are shifted by 0.25 Å from the midway positions. In addition the relative orientation of the static dipole moments of the anions with respect to the monovalent cations is different: In $CdCl_2$, for example, the dipole moments are directed towards the Cr planes. Despite these differences, a "microscopic" lattice-dynamical model for $AgCrS_2$ should include the static dipole moments of the anions. The anisotropy arising from these static dipole moments together with the macroscopic polarization field parallel to the z axis in the pyroelectric phase are expected to be responsible for the large differences in the vibrational frequencies of modes 1 and 2. The application of such a microscopic model to the $AgCrS_2$ structure is, however, very complicated and beyond the scope of this paper. In our phenomenological model the large anisotropy is reflected by the necessity of introducing two widely different short-range force constants for the Ag_2—S_3 bonds (0.40 mdyn/Å) and the Ag_2—$S_{4'}$ bonds (0.03 mdyn/Å) (Table II, Fig. 1). That the force constants of these two bonds will be different is also to be expected from the different bond lengths [$d(Ag_2$—$S_3)=2.36$ Å, $d(Ag_2$—$S_{4'})=2.71$ Å]. The difference in the bond lengths as well as in the force constants is related with the large polarizabilities of the anions and the macroscopic field parallel to the z axis.

The eigenvectors of the modes shown in Figs. 3 and 5–7 depend on the force constants but calculations have shown that this dependence is small and therefore these eigenvectors represent good approximations of the patterns of ionic displacements. A glance at Fig. 7 shows that the intensities of modes

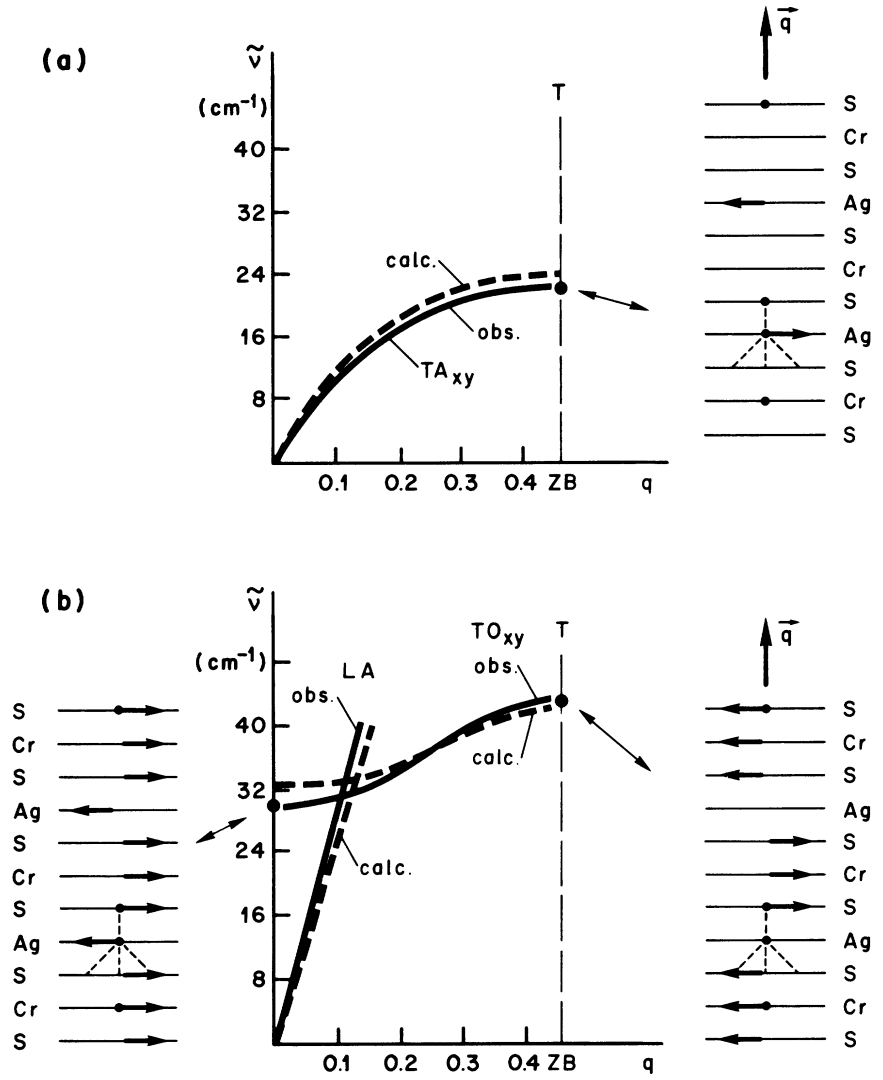

FIG. 5. (a) Dispersion of TA phonons propagating along Γ-T of $AgCrS_2$ at room temperature, and ionic displacements of the zone-boundary mode at the T point. (b) Dispersion of TO and LA phonons propagating along Γ-T; the figure also shows the ionic displacements for the TO modes at the Γ and T points. Dashed lines: rigid-ion model calculation.

3 and 4 are expected to be weak since the sulfur ions move in opposite directions with nearly equal amplitudes resulting in small induced dipole moments. This is the reason for the weak intensity of mode 3 observed in Fig. 2 and for the fact that mode 4 has not been observed at all. On the other hand, the intensity of mode 5, for example, will be very large since in this mode positive and negative charges are moving in opposite directions, leading to a large induced dipole moment, which is in agreement with experiment (Fig. 2). These qualitative statements can be confirmed by calculating the intensities of these modes using the eigenvectors and effective charges. Our model predicts an intensity ratio for modes 3 and 5 of about 6×10^{-3} and for modes 4 and 5 of about 2×10^{-4}. The weak intensity of the z-polarized mode 2 is probably due to preferential orientation of the crystallite in the uniaxially presses pellets.

B. Effective anharmonic potential of the low-frequency infrared-active mode

In this section we discuss the origin of the strong and anomalous temperature dependence of the low-frequency TO mode at $q=0$ (Fig. 4). $AgCrS_2$ shows a magnetic phase transition at $T_N=40$ K.[4] No changes in lattice parameters have been observed at T_N.[3] Furthermore, the change in slope of $\tilde{\nu}(T)$ in Fig. 4 occurs near 200 K. It is therefore highly improbable that the anomaly in $\tilde{\nu}(T)$ is related with the

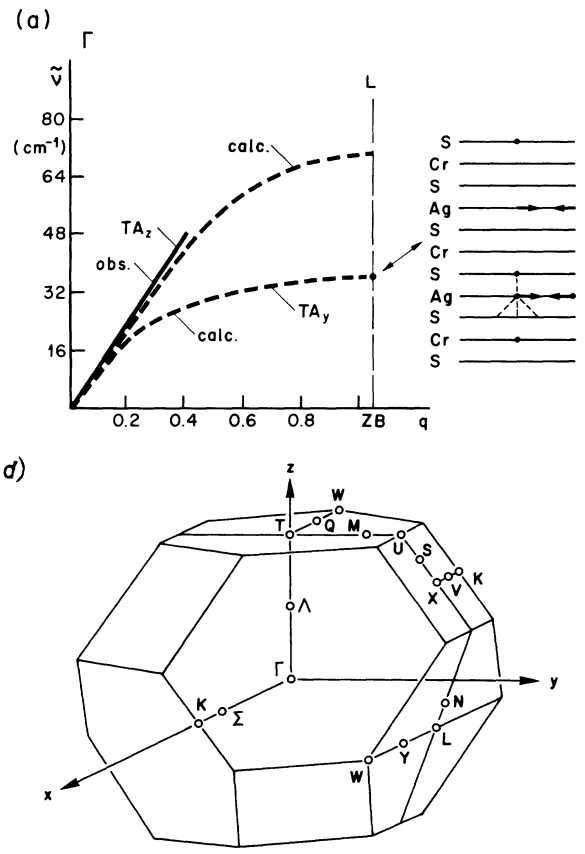

FIG. 6. (a) Dispersion of TA phonons along Γ-L of $AgCrS_2$ at room temperature. Dashed lines: rigid-ion model calculation; the figure also shows the ionic displacements for the low-frequency TA mode at the L point. In this mode neighboring silver ions in a layer are moving in opposite directions and parallel to the xy plane. (b) Brillouin zone for $AgCrS_2$.

magnetic phase transition, but is rather due to strong anharmonicity. In order to show that $\tilde{\nu}(T)$ can be explained by anharmonicity we have adopted an Einstein model by replacing the low-frequency TO branch in Fig. 5(b) by a single horizontal line. On this basis we have calculated the thermal average of the force constant, $\langle\phi(T)\rangle$, for the mode considered. The frequency is then given by

$$\omega^2(T)=\langle\phi(T)\rangle/\mu\ , \tag{3}$$

where $\omega=2\pi c\tilde{\nu}$ and μ is the effective mass. Since according to Fig. 7 the CrS_2 layers move rigidly against the Ag layers parallel to the xy plane in mode 1, the effective mass is taken to be $1/\mu=1/m_{Ag}+1/(m_{Cr}+2m_S)$. The classical thermal average is given by

$$\langle\phi(T)\rangle=\frac{1}{Z}\int\int\frac{\partial^2 W}{\partial r^2}e^{-W(x,y)/kT}dx\,dy\ . \tag{4}$$

Here Z is the partition function and $W(x,y)$ is an effective anharmonic potential energy for the mode considered. $\partial^2W/\partial r^2$ is the curvature that the particle with mass μ is sampling at the point x,y in the radial direction $(r^2=x^2+y^2)$, and $\exp[-W(x,y)/kT]$ is the probability of finding the particle at that point. In $W(x,y)$ the displacements x and y represent the relative displacements of the Ag layers against the CrS_2 layers, thus $x=u_x(Ag)-u_x(CrS_2)$ and $y=u_y(Ag)-u_y(CrS_2)$. $W(x,y)$ must be invariant under the symmetry operations of the site group C_{3v}. A suitable form for $W(x,y)$ which satisifes this condition is the following exponential-type ansatz:

$$\begin{aligned}W(x,y)=&\tfrac{1}{2}a_2(1-e^{-b_2(x^2+y^2)})\\&+a_3(1-e^{-b_3(x^3-3xy^2)})\\&+a_4(1-e^{-b_4(x^2+y^2)^2})\ .\end{aligned} \tag{5}$$

Note that for small displacements $W(x,y)$ represents a Taylor expansion in the basis functions x^2+y^2, x^3-3xy^2, and $(x^2+y^2)^2$. The integrations in Eq. (4) have been performed numerically. A fit by trial and error to the observed $\tilde{\nu}(T)$ is shown in Fig. 4 and gives the following values of the parameters in Eq. (5): $a_2=0.17$ eV, $b_2=1.9$ Å^{-2}; $a_3=0.12$ eV,

TABLE II. Rigid-ion model parameters used to represent the phonon dispersion of $AgCrS_2$ at room temperature. The numbers of the atoms refer to Fig. 1. The effective charges are $q_{Cr}=1.2e$, $q_{Ag}=0.3e$ and $q_S=-0.75e$.

Internal coordinate	Number	Force constant (mdyn/Å)	Internal coordinate	Number	Force constant (mdyn/Å)
Cr_1-$S_{3'}$	3	0.85	S_3-$S_{4'}$	3	0.08
Cr_1-$S_{4'}$	3	0.80	$S_{3'}$-$S_{4'}$	3	0.03
Ag_2-S_3	1	0.40	S-S[a]	6	0.035
Ag_2-$S_{4'}$	3	0.03	Ag-Ag[a]	3	0.025
Cr_1-Ag_2	1	0.035	Cr-Cr[a]	3	0.015

[a]In-plane nearest-neighbor interaction.

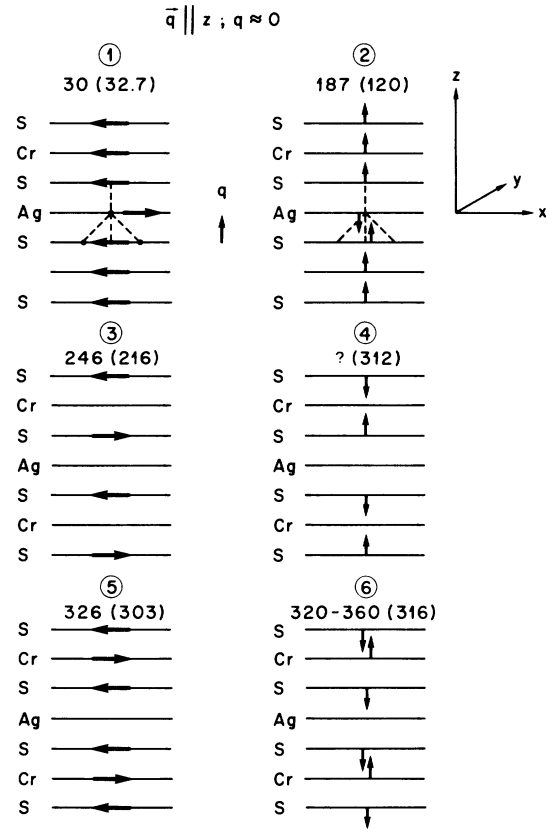

FIG. 7. Patterns of ionic displacements for the $q=0$ modes of $AgCrS_2$ as obtained from the rigid-ion model. In modes 1 and 2 the Cr and S layers move almost rigidly against the *Ag* layers. In modes 3 and 4 the S layers are moving in opposite directions with approximately the same amplitudes leading to small induced dipole moments and hence small infrared intensities. The numbers of the modes refer to Table I. For each mode the observed and calculated (in parentheses) frequencies in units of cm^{-1} are given.

$b_3=0.15$ Å^{-3}, $a_4=0.22$ eV, and $b_4=0.15$ Å^{-4}. The derived potential-energy map is shown in Fig. 8. The function $W(0,y)$ is symmetric: $W(0,y)=W(0,-y)$. On the other hand, $W(x,0)$ is asymmetric and has a Morse-type shape; along the positive x direction the potential increases more slowly ("soft direction") than along the negative x direction ("hard direction"). The positive x direction intersects the face *ABC* of the tetrahedron *ABCD* formed by the four nearest sulfur ions, while the negative x direction intersects its edge *AD*.

The present calculation is classical. From the temperature dependence of the mean occupation number of the mode we expect quantum effects to become appreciable at temperatures below about 20 K. Below this temperature the classical thermal average should be replaced by the corresponding quantum-mechanical expression resulting in a gradual flattening of the $\tilde{\nu}(T)$ curve with a horizontal tangent at $T=0$. In any case, the observed temperature dependence of both the frequency and the large linewidth of this mode reflect a highly anharmonic motion down to about 10 K.

In contrast to the TO mode at the Γ point considered above, the TA mode at the T point [Fig. 5(a)] is temperature independent between 50 and 300 K (Fig. 4). This vibration is therefore practically harmonic, and its effective potential energy is parabolic. In this mode only the silver ions are involved, and the effective mass is therefore equal to m_{Ag}. A comparison between this mode and the TO mode at Γ shows that the two modes have the same relative displacements of the silver ions and thus the same short-range potential. The Coulomb potential, however, is different because in the TA mode silver ions in neighboring planes are moving in opposite directions, while in the TO mode they are moving in the same direction. It is therefore this difference in the Coulomb potential which is responsible for the different temperature dependence of the frequencies of these two modes. A full lattice-dynamical treatment of this problem should be based on a model such as the "self-consistent harmonic approximation".[15] If only the low-frequency acoustic and optic modes were of interest, the CrS_2 layers could be regarded as rigid units. Such an investigation is rather involved and beyond the scope of this paper.

C. Connection of lattice dynamics with ionic conductivity and phase transition

In this paper we have established the existence of very-low-frequency modes in which the silver ions are strongly involved and vibrate parallel to the layers (Figs. 5–7). There are modes in which the silver ions in a layer move all in phase and modes in which neighboring silver ions in a layer move in opposite directions. All these modes contribute strongly to the mean-square displacements of the silver ions and trigger jumps from α to β sites. Very large rms displacements for the silver ions parallel to the layers have indeed been obtained from a refinement of the neutron diffraction data[3]: At 4.2 K the rms value is 0.1 Å and at 300 K it is 0.28 Å. From these data we estimate that the rms displacements for the silver ions at 673 K are at least 0.6 Å, which is comparable to the distance of 0.5 Å between the α site and the point at which the x axis intersects the face *ABC* of the sulfur tetrahedron (Fig. 8).

From steric considerations we expect that in a jump process a silver ion will leave its sulfur tetrahedron through a face rather than through an edge.[19] In Fig. 8 this corresponds to a diffusion

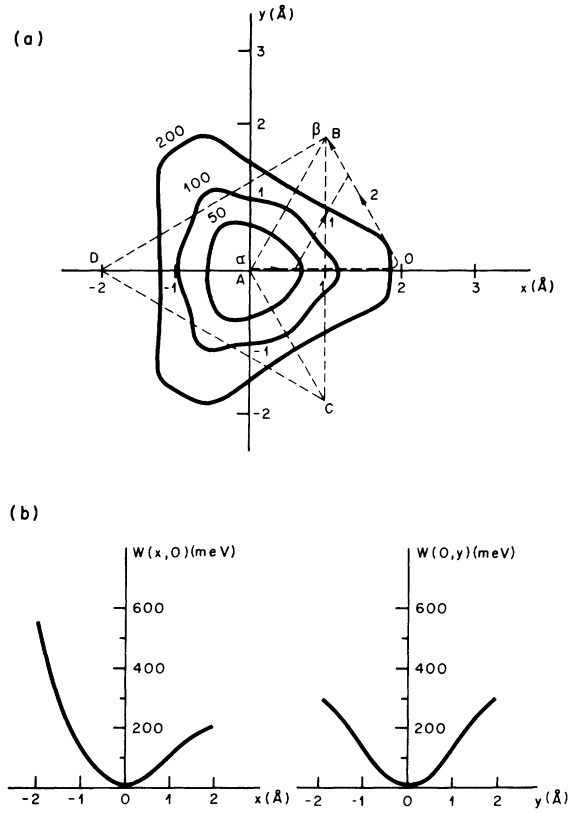

FIG. 8. (a) Energy map of the effective potential $W(x,y)$ derived from the temperature dependence of the low-frequency TO mode at $q=0$ of $AgCrS_2$. The numbers on the equipotential lines indicate the energy in meV, *ABCD* represents the tetrahedron formed by the nearest sulfur ions surrounding a silver ion at the site α. The lines 1 and 2 indicated by ———→—— show possible diffusion paths for a silver ion from the α site to the nearest β site. The point marked O near $x=2$ Å marks an octahedral site. (b) Potential-energy functions $W(x,0)$ and $W(0,y)$.

path which starts along one of the three soft directions, such as the x direction. Once the silver ion has passed through the face *ABC* of its tetrahedron it enters the octahedral space. In Fig. 8 two possible diffusion paths are indicated. In the shorter path 1 the silver ion sneaks around the edge *AB* of the tetrahedron. An indication for this diffusion path comes from the electron density obtained from the x-ray reflections of single crystals above T_c.[8] Path 2 proceeds via the octahedral site in Fig. 8. Such a path cannot be excluded from the electron density data. If the potential energy has a relative minimum at the site O, the Ag ion will vibrate temporarily around this site before jumping to one of the nearest α or β sites. A silver ion at the octahedral site has considerably more space than at the tetrahedral site. We therefore expect that in the octahedral site the force constant and vibrational frequency will be smaller and also more isotropic than in the tetrahedral site. The vibration of the silver ion in the octahedral space could therefore explain the structure observed at high temperatures on the low-frequency side of the absorption shown in Fig. 3. At present it is not possible to make more specific statements about the diffusion path. It should be mentioned that from Fig. 8 we estimate an effective potential barrier for jumps of silver ions of about 0.20 eV. Roughly the same value is obtained from the activation energy deduced from the ionic conductivity.[8]

Independent of its exact trajectory a jump from an α to a β site or to an intermediate octahedral site is always associated with a large displacement component parallel to the xy plane and a small component perpendicular to the xy plane. It is this latter displacement component which with each jump decreases the spontaneous macroscopic polarization of the pyroelectric phase and finally leads to the order-disorder phase transition at $T_c=673$ K. In the absence of the order-disorder transition the strongly temperature-dependent $q=0$ mode could eventually lead to a soft-mode structural phase transition. In reality, however, the premelting of the silver-ion sublattice occurs before the anticipated soft-mode phase transition sets in.

ACKNOWLEDGMENTS

The authors are indebted for many interesting discussions with Dr. L. Pietronero, Dr. S. Strässler, Dr. J. Bernasconi, Dr. H. Neff, and Dr. H. R. Zeller from Brown-Boveri Research Center, as well as with Professor H. Beck, Dr. K. Maschke, Professor R. Orbach, Professor K. A. Müller, and Professor T. M. Rice. We also would like to thank Mr. W. Foditsch for his excellent technical assistance, Mr. Riesterer for his help during the far-infrared measurements, and Mr. St. Bugmann for the preparation of the single crystals.

[1]S. Geller, in *Solid Electrolytes,* Vol. 21 of *Topics in Applied Physics,* edited by S. Geller (Springer, Berlin, 1977), p. 41.

[2]See articles in *Proceedings of the International Conference in Fast Ionic Transport, Gatlinburg, 1981,* edited by J. B. Bates and G. C. Farrington (North-Holland, Amsterdam, 1981), p. 465.

[3]F. M. R. Engelsman, G. A. Wiegers, F. Jellinek, and B. van Laar, J. Solid State Chem. 6, 574 (1973).

[4]P. F. Bongers, C. F. van Bruggen, J. Koopstra, W.P.F.A.M. Omloo, G. A. Wiegers, and F. Jellinek, J. Phys. Chem. Solids 29, 977 (1968).

[5]T. Hibma, in *Intercalation Chemistry,* edited by M. S. Whittingham and A. J. Jacobson (Academic, New York, 1982), p. 285.

[6]T. Hibma, Solid State Ionics 3/4, 203 (1981).

[7]T. Hibma, P. Brüesch, S. Strässler, Solid State Ionics 5, 481 (1981).

[8]T. Hibma, Solid State Commun. 33, 445 (1980).

[9]C. P. Flynn, *Point Defects and Diffusion* (Clarendon, Oxford, 1972).

[10]D. H. Martin and E. Puplett, Infrared Phys. 10, 105 (1969).

[11]P. Brüesch and W. Foditsch, J. Phys. E 12, 872 (1977).

[12]W. Bührer, Nucl. Instrum. Methods 179, 259 (1981).

[13]I. F. Chang, S. S. Mitra, J. N. Plendl, and L. C. Mansur, Phys. Status Solidi 28, 663 (1968).

[14]P. Brüesch, T. Hibma, and W. Bührer, J. Phys. (Paris) 42, Colloq. C6-178, Suppl. 12 (1981).

[15]P. Brüesch, *Phonons: Theory and Experiments I,* Vol. 34 of *Springer Series in Solid-State Sciences,* edited by M. Cardona, P. Fulde, and H. J. Queisser (Springer, Berlin, 1982), p. 175.

[16]H.J.L. van der Valk and C. Haas, Phys. Status Solidi B 80, 321 (1977).

[17]A. Frey and R. Zeyher, Solid State Commun. 28, 435 (1978).

[18]G. Benedek and A. Frey, Phys. Rev. B 21, 2482 (1980).

[19]H. Wiedersich, S. Geller, *The Chemistry of Extended Defects in Non-metallic Solids,* edited by Eyring and M. O'Keefe (North-Holland, Amsterdam, 1969).